

1 **A Post-2013 Drop-off in Total Ozone at Half of Global Ozonesonde Stations: ECC Instrument**
2 **Artifacts?**

3 **Ryan M. Stauffer^{1,2}, Anne M. Thompson², Debra E. Kollonige^{3,2}, Jacquelyn C. Witte^{2*}**
4 **David W. Tarasick⁴, Jonathan Davies⁴, Holger Vömel⁵, Gary A. Morris⁶, Roeland Van**
5 **Malderen⁷, Bryan J. Johnson⁸, Richard R. Querel⁹, Henry B. Selkirk^{10,2}, Rene Stübi¹¹, and**
6 **Herman G. J. Smit¹²**

7 ¹Earth System Science Interdisciplinary Center, University of Maryland, College Park, MD,
8 USA

9 ²Atmospheric Chemistry and Dynamics Lab, NASA/GSFC, Greenbelt, MD, USA

10 ^{*}Now at National Center for Atmospheric Research Earth Observations Laboratory, Boulder,
11 CO, USA

12 ³Science Systems and Applications, Inc., Lanham, MD, USA

13 ⁴Environment and Climate Change Canada, Downsview, ON, CA

14 ⁵National Center for Atmospheric Research Earth Observations Laboratory, Boulder, CO, USA

15 ⁶St. Edwards University, Austin, TX, USA

16 ⁷Royal Meteorological Institute of Belgium, Uccle (Brussels), Belgium

17 ⁸Global Monitoring Division, NOAA Earth System Research Laboratory, Boulder, CO, USA

18 ⁹National Institute of Water & Atmospheric Research (NIWA), Lauder, NZ

19 ¹⁰Universities Space Research Association, Columbia, MD, USA

20 ¹¹Federal Office of Meteorology and Climatology, MeteoSwiss, Aerological
21 Station, Payerne, Switzerland

22 ¹²Institute of Chemistry and Dynamics of the Geosphere: Troposphere, Jülich Research Centre,
23 Jülich, Germany

24

25 Corresponding author: Ryan M. Stauffer (ryan.m.stauffer@nasa.gov)

26 **Key Points:**

- 27 • We report a drop in ozonesonde total column O₃ of 2-8 % relative to independent
28 measurements at nearly half of sites beginning around 2013
- 29 • Comparisons with satellite stratospheric O₃ profiles show the artifact loss peaking at 5-
30 10 % or more in the middle and upper stratosphere

- 31 • Changes in the ozonesonde instrument are associated with the drop-off, but no single
32 factor has been identified as a cause

33 Keywords: ECC Ozonesonde, Aura, OMI, MLS, Suomi-NPP, OMPS

34 Index Terms: 0394, 0365, 9815

35 **Abstract**

36 An international effort to improve ozonesonde data quality and to reevaluate historical
37 records has made significant improvements in the accuracy of global network data. However,
38 during 2013-2016, ozonesonde total column ozone (TCO; O₃) at 17 of 37 regularly reporting
39 stations exhibited a sudden drop-off relative to satellite measurements. The ozonesonde TCO
40 drop is 2-8 % compared to satellite and ground-based TCO, and 5-10 % or more compared to
41 satellite stratospheric O₃ profiles, compromising the use of recent data for trends, although they
42 remain reliable for other uses. Hardware changes in the ozonesonde instrument appear to be a
43 major factor in the O₃ drop-off, but no single property of the ozonesonde explains the findings.
44 The bias remains in recent data. Research to understand the drop-off is in progress; this letter is
45 intended as a caution to users of the data. Our findings underscore the importance of regular
46 ozonesonde data evaluation.

47 **Plain Language Summary**

48 Balloon-borne ozonesondes provide accurate measurements of atmospheric ozone (O₃)
49 from the surface to above 30 km with high vertical resolution. Dozens of global stations have
50 regularly launched ozonesondes for decades, and they provide vital information for improving
51 O₃-measuring satellite algorithms, tracking recovery of the stratospheric O₃ layer, and our
52 understanding of surface to lower stratospheric O₃ changes in an evolving climate. We present
53 the discovery of an apparent instrument artifact that has caused total column O₃ measurements

54 from about half of global stations to drop by 2-8 % starting in 2013-2016, limiting their
55 suitability for calculating O₃ trends. Work is underway to solve the problem, but the exact cause
56 of the drop is still unknown. This letter serves as a caution to the community of ozonesonde data
57 users.

58

59 **1 Background: The Ozonesonde Instrument and Data Quality Assurance**

60

61 The electrochemical concentration cell (ECC) ozonesonde measures ozone (O_3) profiles
62 from the surface through the mid-stratosphere (~ 5 hPa). Ozone is measured via a chemical
63 reaction from bubbling ambient O_3 into two electrochemical cells containing a potassium iodide
64 (KI) solution (sensing solution type or SST). The ECC is launched on a weather balloon in
65 tandem with a radiosonde that transmits O_3 partial pressure simultaneously with pressure,
66 temperature, humidity (PTU), and GPS-derived wind data to a ground station approximately
67 once a second. With a 20-30 s response time, the effective vertical resolution of the O_3 signal is
68 ~ 150 m.

69 Because each ozonesonde is a new instrument that must be prepared before launch, it is
70 essential to standardize instrument preparation, operations, and the treatment of raw data. In the
71 past decade, a panel of researchers have engaged in both individual and collective tests of
72 instrumentation, meeting regularly to discuss quality assurance and to develop standard operating
73 procedures (SOP) in an activity designated Assessment of SOP for Ozonesondes (ASOPOS).
74 Current SOP were published in **Smit and ASOPOS (2014)**. The main sources of instrument
75 variability are the instrument type (there are two major manufacturers of ECC instruments,
76 which we call “Type1” and “Type2”), the composition of the SST, conditioning protocol, and
77 post-processing; these parameters are given in the metadata for each record.

78 ASOPOS has also published guidelines for reprocessing sonde data records that may be
79 affected by deliberate or inadvertent ECC preparation changes. Case in point: the ASOPOS
80 recommendation is to deploy each ECC type with a different SST, even though the two types
81 operate on the exact same measurement principle. If a station changes only one of these

82 variables, the resulting step change in O₃ is considered an instrumental artifact. Reprocessing is
83 carried out to compensate for such changes, and the data are said to be homogenized (**Smit and**
84 **ASOPOS, 2012; Deshler et al., 2017**). Both the SOP and reprocessing guidelines are based on
85 laboratory (**Smit et al., 2007**) and field tests (**Deshler et al., 2008**) in which different sensors are
86 compared with a standard O₃ reference photometer. In the lab, tests are made with 2-4 ECC
87 sensors operating in a closed chamber that simulates a standard profile over a 2-hr “flight.” Field
88 tests compare instruments on a single gondola launched with a special balloon.

89 During the period 2013 through 2017 data from more than 25 ozonesonde stations were
90 reprocessed (**Tarasick et al., 2016; Van Malderen et al., 2016; Thompson et al., 2017; Witte**
91 **et al., 2017; Sterling et al., 2018; Witte et al., 2019**). In general, reprocessed data show
92 significant improvements in comparisons to independent total column ozone (TCO)
93 measurements. Reprocessed data at 12 of 14 SHADOZ stations agree to within 2 % of satellite
94 and ground-based TCO measurements (**Thompson et al., 2017**), compared to > 8 % offsets at
95 half of the stations through 2004 in **Thompson et al. (2007)**. Improvements in tropical mid-
96 stratospheric O₃ readings also led to better agreement with MLS profiles (2005-2017; **Witte et**
97 **al., 2017**).

98 In spite of the reprocessing successes, the homogenized data for two tropical stations
99 (Costa Rica and Hilo) displayed sharp 5 % drop-offs in TCO relative to satellite measurements
100 after 2014; at Hilo a simultaneous discrepancy appeared relative to the Mauna Loa Dobson
101 spectrometer (**Thompson et al., 2017; Sterling et al., 2018**). The drop-off was also observed in
102 the original datasets, ruling out the reprocessing as the cause. Furthermore, NOAA’s Boulder,
103 CO, site, which used the same instrumentation and SST, did not appear to be similarly affected.
104 Hypothesized causes for these findings, e.g., hardware changes in the 2011-2016 period (the

105 company manufacturing Type1 ECCs changed ownership twice) or NOAA’s non-standard SST
106 used at the above-mentioned sites, were tested along with other variables in a new series of
107 chamber tests (JOSIE; Jülich Ozonesonde Intercomparison Experiments) in late 2017. Initial
108 results from the 80 chamber profiles in JOSIE-SHADOZ could not explain the drop-off behavior
109 (**Thompson et al., 2019**), and the cause remained unsolved.

110 Because ozonesonde profiles are relied upon as the foundation for satellite O₃ retrievals
111 and validation, we re-examine the agreement among sonde, satellite, and ground-based TCO
112 with two more years of data from the SHADOZ and NOAA networks to determine if the drop-
113 offs reported in **Thompson et al. (2017)** and **Sterling et al. (2018)** persist. We also extend these
114 analyses to the global network during the Aura satellite era of October 2004 to present. We find
115 that about half of these 37 stations exhibit an instrumental artifact drop-off in TCO after 2013,
116 with a coincident decline in stratospheric O₃. Instrumental factors are investigated but no
117 definitive explanation for these findings has yet emerged. In **Section 2** data sources and
118 statistical methods are described. **Section 3** describes results and potential changes to the ECC
119 instrument and factors that require further investigation. **Section 4** is a summary and
120 recommendations for use of data affected by the ECC O₃ drop-off.

121

122 **2 Data and Methods**

123

124 **2.1 ECC Ozonesonde Data**

125

126 We selected a total of 37 global ECC ozonesonde sites based on the availability of
127 consistent and up-to-date records during the Aura period of October 2004 to present (i.e. data

128 available within the last few years; an exception is Watukosek which ended in October 2013) to
129 analyze the recent drop in ECC TCO measurements. Currently, 28 of the sites launch Type1
130 ECCs, and nine launch Type2. Some sites have previously changed ECC types, SST, or both, so
131 the most recent metadata are listed in **Table 1**. The primary evaluation of ozonesonde data is
132 with NASA's Aura satellite; sample numbers listed in **Table 1** are from the Aura period only.
133 None of the ozonesonde data here are normalized to a TCO measurement or an outside data
134 source.

135

136 **2.2 Satellite and Ground-Based Data**

137

138 Satellite TCO measurements are from the Aura Ozone Monitoring Instrument (OMI;
139 **McPeters et al., 2008**) and the Suomi-NPP Ozone Mapping Profiler Suite (OMPS; **McPeters et**
140 **al., 2019**). Stratospheric O₃ profile measurements are from the Aura Microwave Limb Sounder
141 (MLS; **Froidevaux et al., 2008**). To identify “coincident” satellite overpasses, we limit Level 2
142 TCO data to within 8 hours of the ozonesonde measurement. We use MLS v4.2 Level 2 O₃ data
143 averaged within one day and 5° latitude and 8° longitude of the ozonesonde launch. MLS data
144 are screened according to the v4.2 Level 2 MLS Data Quality document (**Livesey et al., 2018**).
145 Sensitivity tests on our screening of coincident satellite TCO data by limiting comparisons based
146 on cloud fraction or overpass distance to the ECC site had negligible effects on the statistics (less
147 than 1 % change in overall OMI/ECC TCO agreement).

148 The OMI and OMPS TCO measurements compare well with the series of Solar
149 Backscatter Ultraviolet instruments and are suitable for TCO trends analysis (**McPeters et al.,**
150 **2015; 2019**). Aura MLS O₃ measurements in the stratosphere exhibit little drift – the v3.3

151 measurements are stable to within 1.5 % per decade (**Hubert et al. 2016**; it is presumed the v4.2
152 data used here have similar stability). Thus, these three satellite instruments are suitable to detect
153 significant changes in the ECC ozonesonde network. Our primary ECC comparisons are with
154 OMI because of its > 15 year record. OMPS and MLS reinforce the OMI results.

155 A total 23 of the 37 ECC sites have a co-located ground-based TCO instrument (**Table**
156 **1**). Most sites have a Brewer or Dobson spectrophotometer (or both at Hilo and Tatenou); Réunion
157 uses a SAOZ UV-visible spectrometer. ECC TCO comparisons with all three ground-based
158 instrument types are found in **Thompson et al. (2017)**.

159

160 **2.3 Defining the ECC O₃ Drop-off: Example Sites**

161

162 To characterize the O₃ drop-off, we separate the sites with unambiguous drops in TCO,
163 which we call “affected” sites, from those called “reference” sites. Affected sites are defined as
164 those recording drops of TCO relative to OMI of greater than 2 % after visually locating a
165 downward step-change in the time series of comparisons with OMI. This does not mean there is
166 no change at the reference sites; a < 2 % drop-off is assumed to be less significant. The TCO
167 drop is calculated as the difference in mean bias compared to OMI TCO before (Oct. 2004 to
168 drop-off date) and after the drop-off date (through the end of the site’s ECC record). For
169 example, **Figure 1a** displays a sudden TCO drop-off relative to OMI at Kelowna in March 2015.
170 The ECC TCO averaged 4.0 % higher than OMI before the drop-off in March 2015 (564
171 samples), and -0.4 % lower than OMI after March 2015 (100 samples) – a 4.4 % drop, meeting
172 the > 2 % criterion. The visual identification of the drop-off date is subjective, but objective
173 analyses of ECC serial numbers follow in Section 3.3.

174 The drop-off emerged at Nairobi in June 2015, and at Lauder in September 2016 (**Figure**
175 **1b, c**). Nairobi and Lauder both exhibit drop-offs of 2.2 % relative to OMI. The percent
176 differences between ozonesonde and MLS stratospheric O₃ in the top panels of **Figure 1** show
177 that the drop in ECC O₃ relative to MLS is coincident with the TCO drop.

178

179 **3 Results and Discussion**

180

181 **3.1 Sites Affected by the ECC O₃ Drop-off**

182

183 Using the criterion of a > 2 % TCO drop relative to OMI, we find that 17 of 37 sites are
184 affected by a sudden TCO drop-off. **Table 1** lists the affected sites in bold including the TCO
185 drop relative to OMI. A map of all sites examined, with affected sites colored according to the
186 magnitude of TCO drop-off, is shown on **Figure 2**. Defining the drop in TCO as relative to OMI
187 is necessary considering that some sites previously exhibited a high bias compared to satellites,
188 with the drop-off leading to better agreement with OMI (e.g. Kelowna in **Figure 1a**).

189 Dates of the first notable drop in TCO measurements range from August 2013 at San
190 Cristóbal to January 2017 at American Samoa. All but one (Natal) of the affected sites are Type I
191 sites. The magnitude of the TCO drop-off varies considerably. The drop in TCO at Lauder is a
192 relatively modest -2.2 %, whereas changes of -7.5 % and -8.2 % are observed at Churchill and
193 Yarmouth.

194 Comparisons similar to **Figure 1** for the remaining 34 sites in **Table 1** are found in the
195 Supplementary Material in **Figures S1a-n and S2a-t**. We note that sites show periods of high or
196 low bias compared to OMI and MLS (e.g. Madrid's high bias for a portion of 2009; **Figure S2g**),

197 but our focus is on sudden drops in O₃ that persist for more than 2 or 3 years in the most recent
198 record.

199 The three Japanese stations examined do not exhibit a drop in ECC TCO. Out of 10
200 SHADOZ stations that are currently launching Type1 ECCs, only Réunion Island and Kuala
201 Lumpur are not affected. Note that, for reasons unknown, Kuala Lumpur has measured
202 consistently low O₃ since the beginning of the Aura record in late 2004. In summary, there is
203 inconsistency in TCO drop-off amount, and the drop-off is not a universal problem.

204

205 **3.2 Comparisons with Aura MLS Stratospheric O₃**

206

207 A closer examination of ECC and MLS stratospheric O₃ comparisons is warranted given
208 the coincidence between the OMI and OMPS TCO drop-off, and apparent MLS O₃ drop-off in
209 **Figure 1. Figure 3** shows a composite of comparisons between MLS and ECC ozonesonde
210 stratospheric O₃ at the 17 affected sites before and after the identified drop-off (dates in **Table**
211 **1**). Prior to the drop-off at the 17 affected ECC sites, stratospheric O₃ biases compared to MLS
212 follow the zero line in **Figure 3** (blue colors). After the drop-off in TCO, the ECC measurements
213 shift 5-10 % or more lower relative to MLS (red colors), occasionally reaching > 20 % low
214 above 10 hPa (the 25th percentile value at the 6.81 hPa MLS level is -23.0 %). **Figure 3** shows
215 that the stratospheric O₃ drop-off is the major contributor to the TCO offsets with OMI and
216 OMPS. At this point, a similar drop-off in tropospheric O₃ has not been detected and is presumed
217 to be insignificant. Exceptions are two stations, Costa Rica and Hilo, which may be reading low
218 in recent years in the troposphere due to volcanic SO₂ interference (e.g. **Morris et al., 2010**).
219 That is beyond the scope of our study.

220

221 **3.3 Potential ECC Instrument Factors in the O₃ Drop-off**

222

223 The ECC O₃ drop-off has been quantified against satellite TCO, satellite O₃ profiles, and
224 ground-based instruments (**Thompson et al., 2017; Sterling et al., 2018**; ground-based
225 comparisons to follow in Section 3.5). Thus, we rule out geophysical factors as a cause; the drop-
226 off is an instrument artifact, so we consider potential instrumental contributions. Each ECC is
227 built from a number of components that may change over time as the manufacturers' suppliers
228 change. For example, the Type1 instrument changed manufacturer twice between 2011 and
229 2016. Components include the cells holding the SST, the ion bridge between the two cells, the
230 air intake pump, the constant-speed motor, batteries, and the platinum electrodes. A 2-8 %
231 change of response could be caused by loss of O₃ or of molecular iodine, losses through the
232 internal resistance of the cell, or in-flight changes in the pump and motor efficiency. The SST
233 composition and the radiosonde model (and interface) are additional considerations (Section
234 3.6). The ECC serial number is used to evaluate potential instrument or component changes over
235 time.

236 **Figure 4** shows histograms of ECC TCO offsets with OMI and OMPS separated by the
237 16 affected (red on **Figure 4**) and 12 reference (blue on **Figure 4**) Type1 sites. Each histogram
238 displays statistics for every 1000 serial numbers (e.g. 24K = 24000-24999). The affected sites
239 show a low bias for 25K serial numbers, abruptly dropping from a median TCO bias compared
240 to OMI and OMPS of +0.7 % (24K), to -2.9 % (25K). The reference sites show no such drop,
241 and, in fact, no recent serial number set since 24K has a median bias larger than -1.2 % (30K) for
242 the 12 reference sites. The affected sites show significant negative biases for all serial numbers

243 from 25K to 35K, with a maximum median low bias of -5.1 % for 31K serial numbers.
244 Histograms for *all* serial numbers at affected (**Figure S3**) and reference (**Figure S4**) Type1 sites
245 are found in the Supplementary Material. **Figure S3** shows the history of good ECC/satellite
246 agreement at affected Type1 sites throughout the Aura record since October 2004 and prior to
247 the 25K serial numbers, although there are indications of some low-biased measurements from
248 serial numbers 20-22K. The largest deviation for reference Type1 sites is the +2.1 % median bias
249 for 16K serial numbers (**Figure S4**). In summary, before the TCO drop-off at the affected sites,
250 the ECC TCO comparisons with satellite measurements averaged within 1 or 2 %, and
251 comparisons at reference sites remain, on average, within 1 or 2 %.

252 Reference and affected Type1 sites were both launching ECCs with similar serial
253 numbers, so it is puzzling why they show such large discrepancies in their comparisons with
254 satellite TCO. **Figure S5** shows a continuous time series of Type1 serial numbers and TCO
255 comparisons with OMI and OMPS, which illustrates the consistent unbiased TCO values at
256 reference sites (**Figure S5a**), and the large drop-off at affected sites (**Figure S5b**). This
257 commingling of good and poorly-performing Type1 serial numbers, which appear to be
258 distinguishable only by site, suggests that the ECC O₃ drop-off is not due to manufacturing
259 issues for the Type1 ECC alone and that at least one additional secondary factor must play a role
260 in the occurrence of this issue.

261

262 **3.4 Stations with Type2 ECCs**

263

264 We examined nine Type2 ECC ozonesonde sites for a drop-off and sudden low TCO
265 bias. Histograms of the TCO offset between reference Type2 ECCs and OMI and OMPS are

266 shown in **Figure S6** with the serial numbers grouped by 1000 as in **Figure 4**. Note that the
267 similar serial numbers between Type1 and Type2 ECCs are purely a coincidence. The Type2
268 histograms show no abrupt downward shift in agreement with satellite TCO as seen at the
269 affected Type1 sites in **Figure 4 and Figure S3**. An exception is at Natal.

270

271 **3.5 ECC Comparisons with Ground-Based TCO Measurements**

272

273 Of the 37 sites analyzed here, 23 have ground-based TCO measurements to compare
274 against the ECCs (**Table 1**). Example time series of the comparisons between ECCs and the
275 Brewer at Churchill, and the Brewer and Dobson at Hilo are shown in **Figure S7**. The ground-
276 based TCO measurements near Hilo are taken at Mauna Loa (3405 m), which explains why the
277 ECC TCO is higher than the Brewer and Dobson prior to the August 2014 drop-off. Histograms
278 similar to **Figure 4 and Figures S3, S4, and S6** for the ground-based TCO comparisons are
279 shown in **Figures S8-S10**. The ECC TCO drop-off relative to the ground-based instruments is
280 ~3-4 % after Type1 24K serial numbers in **Figure S8**. The ground-based comparisons with
281 reference Type1 and Type2 sites (**Figures S9 and S10**) are quite variable, but no sustained drop-
282 off is apparent as observed in **Figure S8**.

283

284 **3.6 Possible Sources of the Drop-Off**

285

286 Around 2010-2012, most of the affected ozonesonde sites examined here switched from
287 the Vaisala RS-80 to RS-92 radiosonde, or from RS-80 to the InterMet iMet radiosonde. The
288 radiosonde pressure measurements affect the ECC O₃ calculation and altitude registration, so a

289 change from non-GPS RS-80 to GPS-enabled RS-92 and iMet radiosondes can lead to pressure
290 measurement changes, which translate to O₃ changes (**Stauffer et al., 2014**). Some sites (e.g.
291 Lauder in 2015) switched radiosondes again from RS-92 to the RS-41. An example of an RS-80
292 to iMet transition at Hilo is shown in **Figure S11**. There is a shift in mid-stratospheric pressure
293 and temperature measurements with the transition to iMet in 2011-2012, but this change occurs
294 two years before the Hilo low O₃ bias in August 2014. Similar mismatches between radiosonde
295 changes and the ECC drop-off are found at other sites. Costa Rica switched from RS-80 to iMet
296 radiosondes in 2012-2013, but the drop-off did not occur until January 2016 (**Thompson et al.,**
297 **2017**). Nairobi switched from RS-80 to RS-92 radiosondes in 2010, but there was no drop-off
298 until June 2015. We therefore rule out radiosonde changes as the primary cause of the ECC O₃
299 drop-off.

300 The drop-off is found at sites that use a variety of SSTs (**Table 1**) and three different
301 radiosonde types (RS-92 or 41 and iMet). Sites that are seemingly unaffected, e.g. Trinidad
302 Head, Boulder, and Huntsville, all use the same 1.0 % KI with 1/10th buffer SST and iMet
303 radiosonde combination as Hilo and Costa Rica (**Figure S1h, S1i**). We have not fully explored
304 the effects of different SSTs on the O₃ drop-off, but given that all three SSTs currently in use are
305 affected (**Table 1**), it does not appear that SST is a major factor.

306 The ASOPOS 2.0 panel will perform additional experiments and analyses to identify
307 possible sources of the O₃ drop-off. Candidate tests include examining the different radiosonde
308 interface boards and batteries used on Type1 ECC sondes, reviewing site ECC preparation
309 procedures, testing ECC pump performance in flight and in vacuum chambers, and experiments
310 with older Type1 ECCs manufactured before the drop-off began. Both Type1 and Type2
311 ozonesondes, four different sensing SSTs, and varying preparation procedures were tested in the

312 2017 JOSIE-SHADOZ experiment (**Thompson et al., 2019**). In-depth analysis of the 80 profiles
313 from JOSIE-SHADOZ should help identify the causes and magnitudes of contributing factors
314 like SST to the ECC O₃ drop-off.

315

316 **4 Summary and Recommendations for Affected Data**

317

318 Since 2013-2016, we observed a drop-off in ECC ozonesonde TCO and stratospheric O₃
319 at 17 ECC global ozonesonde sites, 16 of which launch Type1 ECC ozonesondes. The TCO drop
320 is 2-8 % compared to OMI TCO measurements, and the stratospheric O₃ drop can be greater than
321 10 % compared to MLS O₃ profiles in the mid-stratosphere. The low bias is notably absent at
322 almost half of the 28 Type1 sites that we examined. Except for Natal, there is no significant
323 drop-off or change in bias for Type2 ECC ozonesondes during similar years. Because the drop-
324 off varies greatly from site-to-site, it seems likely that it is influenced by station-specific
325 procedures yet to be identified; the ECC O₃ drop-off probably has more than one single cause.

326 Affected data archives such as SHADOZ (<https://tropo.gsfc.nasa.gov/shadoz/>), the World
327 Ozone and Ultraviolet Data Centre (WOUDC.org), and the Network for the Detection of
328 Atmospheric Composition Change (NDACC; ndaccdemo.org) are posting caveats and flagging
329 affected profiles. Ongoing research is directed at identifying the cause of the low O₃ bias.

330 We emphasize that all reprocessed data are more accurate than unhomogenized data. For
331 affected sites, data before the drop-off are highly reliable and even affected data are accurate for
332 satellite validation and algorithms, process studies, and model evaluation because the apparent
333 drop-off averages less than 5 %. However, the affected data are not appropriate for calculations
334 of TCO or above-50-hPa stratospheric trends or satellite drift.

335

336 **Acknowledgments**

337 Funding for this work was provided through support of SHADOZ by the NASA Upper Air
338 Research Program (UARP; Dr. Kenneth Jucks program manager) to NASA/GSFC (A. M.
339 Thompson, PI). SHADOZ ozonesonde data were downloaded from the NASA/GSFC archive at
340 <https://tropo.gsfc.nasa.gov/shadoz/>. Canadian reprocessed ozonesonde data were provided by co-
341 author D. Tarasick, and reprocessed Uccle ozonesonde data were provided by co-author R. Van
342 Malderen. NOAA ozonesonde data (Boulder, Huntsville, and Trinidad Head) were downloaded
343 at <ftp://aftp.cmdl.noaa.gov/data/ozwv/Ozonesonde/>. All other ozonesonde data and all ground-
344 based TCO data are available at the World Ozone and Ultraviolet Data Centre (WOUDC;
345 <https://woudc.org/data/explore.php?lang=en>). Aura MLS v4.2 Level 2 O₃ overpass data were
346 downloaded at <https://avdc.gsfc.nasa.gov/pub/data/satellite/Aura/MLS/V04/L2GPOVP/O3/>.
347 OMI and OMPS Level 2 TCO overpass data were downloaded at
348 <https://avdc.gsfc.nasa.gov/pub/data/satellite/Aura/OMI/V03/L2OVP/OMTO3/> and
349 https://avdc.gsfc.nasa.gov/pub/data/satellite/Suomi_NPP/L2OVP/NMTO3-L2/.

350

351 **References**

352 Deshler, T., et al. (2008), Atmospheric comparison of electrochemical cell ozonesondes from
353 different manufacturers, and with different cathode solution strengths: The Balloon
354 Experiment on Standards for Ozonesondes, *J. Geophys. Res.*, 113, D04307,
355 doi:10.1029/2007JD008975.

356 Deshler, T., R. Stuebi, F. J. Schmidlin, J. L. Mercer, H. G. J. Smit, B. J. Johnson, R. Kivi, R., and
357 B. Nardi (2017), Methods to homogenize electrochemical concentration cell (ECC)
358 ozonesonde measurements across changes in sensing solution concentration or ozonesonde
359 manufacturer, *Atmos. Meas. Tech.*, 10, 2021–2043, doi:10.5194/amt-10-2021-2017.

360 Froidevaux, L., et al. (2008), Validation of Aura Microwave Limb Sounder stratospheric ozone
361 measurements, *J. Geophys. Res.*, 113, D15S20, doi:10.1029/2007JD008771.

362 Hubert, D., et al. (2016), Ground-based assessment of the bias and long-term stability of 14 limb
363 and occultation ozone profile data records, *Atmos. Meas. Tech.*, 9, 2497–2534,
364 <https://doi.org/10.5194/amt-9-2497-2016>.

365 Livesey, N. J., et al. (2018), Version 4.2x-3.1 Level 2 data quality and description document, JPL
366 D-33509 Rev. B. [Available at [https://mls.jpl.nasa.gov/data/v4-
367 2_data_quality_document.pdf](https://mls.jpl.nasa.gov/data/v4-2_data_quality_document.pdf).]

368 McPeters, R., Kroon, M., Labow, G., Brinksma, E., Balis, D., Petropavlovskikh, I., Veefkind, J.
369 P., Bhartia, P. K., and Levelt, P. F. (2008), Validation of the Aura Ozone Monitoring
370 Instrument total column ozone product, *J. Geophys. Res.*, 113, D15S14,
371 doi:10.1029/2007JD008802.

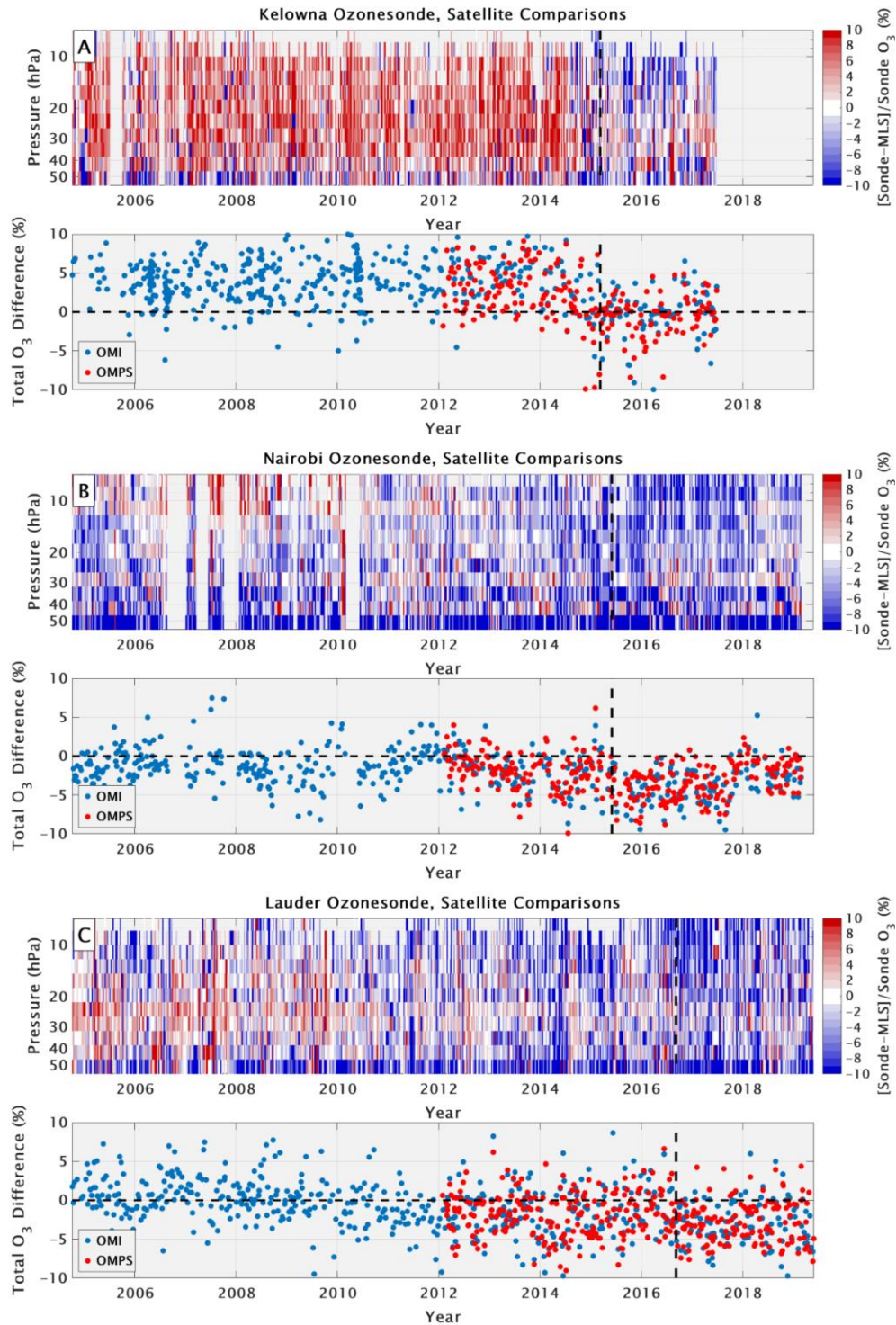
- 372 McPeters, R. D., Frith, S., and Labow, G. J. (2015), OMI total column ozone: extending the
373 long-term data record, *Atmos. Meas. Tech.*, 8, 4845–4850, [https://doi.org/10.5194/amt-8-](https://doi.org/10.5194/amt-8-4845-2015)
374 4845-2015.
- 375 McPeters, R., Frith, S., Kramarova, N., Ziemke, J., and Labow, G. (2019), Trend quality ozone
376 from NPP OMPS: the version 2 processing, *Atmos. Meas. Tech.*, 12, 977–985,
377 <https://doi.org/10.5194/amt-12-977-2019>.
- 378 Morris, G. A., W. D. Komhyr, J. Hirokawa, J. Flynn, B. Lefer, N. Krotkov, F. Ngan (2010), A
379 balloon sounding technique for measuring SO₂ plumes, *J. Atmos. Oceanic Technol.*, 27,
380 1318–1330. doi: 10.1175/2010JTECHA1436.1
- 381 Smit, H. G. J., et al. (2007), Assessment of the performance of ECC-ozonesondes under quasi-
382 flight conditions in the environmental simulation chamber: Insights from the Jülich Ozone
383 Sonde Intercomparison Experiment (JOSIE), *J. Geophys. Res.*, 112, D19306,
384 doi:10.1029/2006JD007308.
- 385 Smit, H. G. J., and the Panel for the Assessment of Standard Operating Procedures for
386 Ozonesondes (ASOPOS) (2012), Guidelines for homogenization of ozonesonde data,
387 SI2N/O3S-DQA activity as part of “Past changes in the vertical distribution of ozone
388 assessment”. [Available at [http://www-](http://www-das.uwyo.edu/%7Edeshler/NDACC_O3Sondes/O3s_DQA/O3S-DQA-Guidelines%20Homogenization-V2-19November2012.pdf)
389 [das.uwyo.edu/%7Edeshler/NDACC_O3Sondes/O3s_DQA/O3S-DQA-](http://www-das.uwyo.edu/%7Edeshler/NDACC_O3Sondes/O3s_DQA/O3S-DQA-Guidelines%20Homogenization-V2-19November2012.pdf)
390 [Guidelines%20Homogenization-V2-19November2012.pdf](http://www-das.uwyo.edu/%7Edeshler/NDACC_O3Sondes/O3s_DQA/O3S-DQA-Guidelines%20Homogenization-V2-19November2012.pdf).]
- 391 Smit, H. G. J., and the Panel for the Assessment of Standard Operating Procedures for
392 Ozonesondes (ASOPOS) (2014), Quality assurance and quality control for ozonesonde
393 measurements in GAW, World Meteorological Organization, GAW Report 201. [Available
394 at http://www.wmo.int/pages/prog/arep/gaw/documents/FINAL_GAW_201_Oct_2014.pdf.]

- 395 Stauffer, R. M., G. A. Morris, A. M. Thompson, E. Joseph, G. J. R. Coetzee, and N. R. Nalli
396 (2014), Propagation of radiosonde pressure sensor errors to ozonesonde measurements,
397 *Atmos. Meas. Tech.*, 7, 65–79, doi:10.5194/amt-7-65-2014.
- 398 Sterling, C. W., Johnson, B. J., Oltmans, S. J., Smit, H. G. J., Jordan, A. F., Cullis, P. D., et al.
399 (2017). Homogenizing and estimating the uncertainty in NOAA’s long term vertical ozone
400 profile records measured with the electrochemical concentration cell ozonesonde. *Atmos.*
401 *Meas. Tech.*, 11, 3661-3687, <https://doi.org/10.5194/amt-2017-397>
- 402 Tarasick, D. W., J. Davies, H. G. J. Smit, and S. J. Oltmans (2016), A re-evaluated Canadian
403 ozonesonde record: Measurements of the vertical distribution of ozone over Canada from
404 1966 to 2013, *Atmos. Meas. Tech.*, 9, 195–214, doi:10.5194/amt-9-195-2016.
- 405 Thompson, A. M., J. C. Witte, H. G. J. Smit, S. J. Oltmans, B. J. Johnson, V. W. J. H. Kirchhoff,
406 and F. J. Schmidlin (2007), Southern Hemisphere Additional Ozonesondes (SHADOZ)
407 1998–2004 tropical ozone climatology: 3. Instrumentation, station-to-station variability, and
408 evaluation with simulated flight profiles, *J. Geophys. Res.*, 112, D03304,
409 doi:10.1029/2005JD007042.
- 410 Thompson, A. M., Witte, J. C., Sterling, C., Jordan, A., Johnson, B. J., Oltmans, S. J., et al.
411 (2017). First reprocessing of Southern Hemisphere Additional Ozonesondes (SHADOZ)
412 profiles (1998-2016). 2. Comparisons with satellites and ground-based instruments, *J.*
413 *Geophys. Res. Atmos.*, 122, 13000-13025, <https://doi.org/10.1002/2017JD27406>
- 414 Thompson, A. M., H. G. J. Smit, J. C. Witte, R. M. Stauffer, B. J. Johnson, G. Morris, et al.
415 (2019), Ozonesonde quality assurance: The JOSIE-SHADOZ (2017) Experience, *Bull. Amer.*
416 *Met. Soc.*, 100 (1), 155-171, <https://doi.org/10.1175/BAMS-D-17-0311.1>

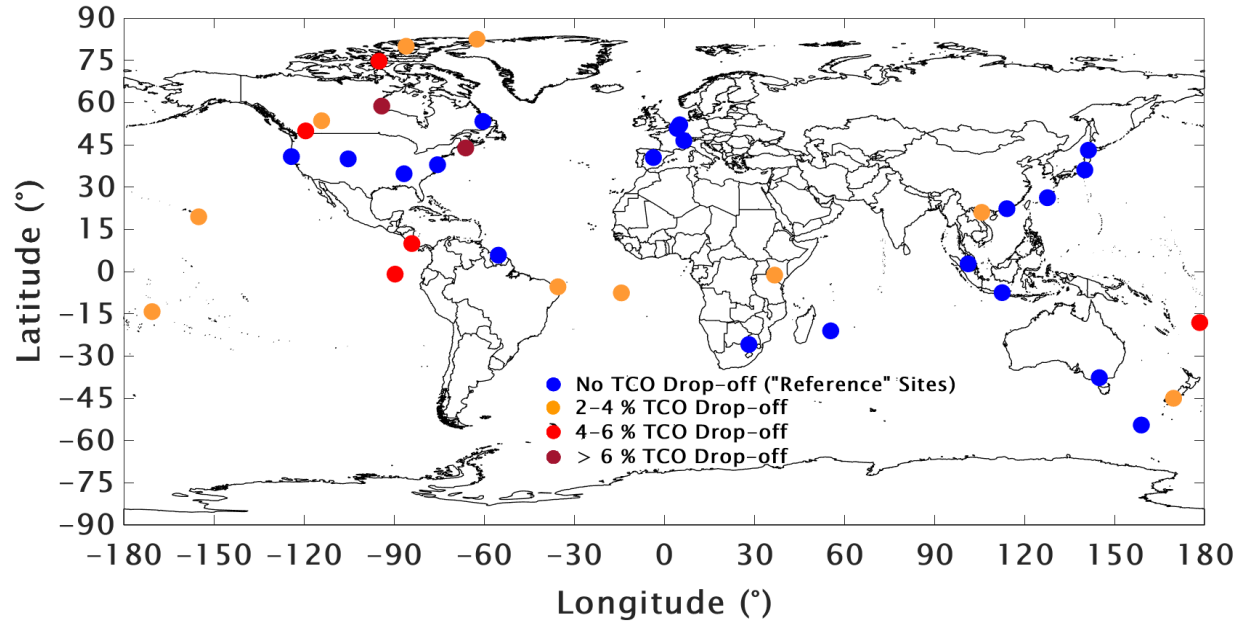
- 417 Van Malderen, R., Allaart, M. A. F., De Backer, H., Smit, H. G. J., and De Muer, D. (2016). On
418 instrumental errors and related correction strategies of ozonesondes: Possible effect on
419 calculated ozone trends for the nearby sites Uccle and De Bilt. *Atmos. Meas. Tech.*, 9, 3793–
420 3816. <https://doi.org/10.5194/amt-9-3793-2016>.
- 421 Witte, J. C., Thompson, A. M., Smit, H. G. J., Fujiwara, M., Posny, F., Coetzee, G. J. R., et al.
422 (2017). First reprocessing of Southern Hemisphere ADditional Ozone-sondes (SHADOZ)
423 profile records (1998–2015): 1. Methodology and evaluation. *J. Geophys. Res. Atmos.*, 122,
424 6611–6636. <https://doi.org/10.1002/2016JD026403>.
- 425 Witte, J. C., Thompson, A. M., Schmidlin, F. J., Northam, E. T., Wolff, K. R., and Brothers, G.
426 B. (2019). The NASA Wallops Flight Facility digital ozonesonde record: Reprocessing,
427 uncertainties, and dual launches. *Journal of Geophysical Research: Atmospheres*, 124, 3565–
428 3582. <https://doi.org/10.1029/2018JD030098>
429

430 Table 1. ECC type, total samples, lat/lon, KI solution type (SST), the 25th percentile, mean, and
 431 75th percentile TCO differences with OMI (October 2004–present), date and amount of drop-off
 432 if applicable, and ground-based instrument if applicable are listed. Sites with a > 2 % drop in
 433 TCO relative to OMI (Section 2.3) are in bold. Type1 is EnSci (Westminster, CO, USA) and
 434 Type2 is Science Pump Corporation (SPC; Camden, NJ, USA).
 435

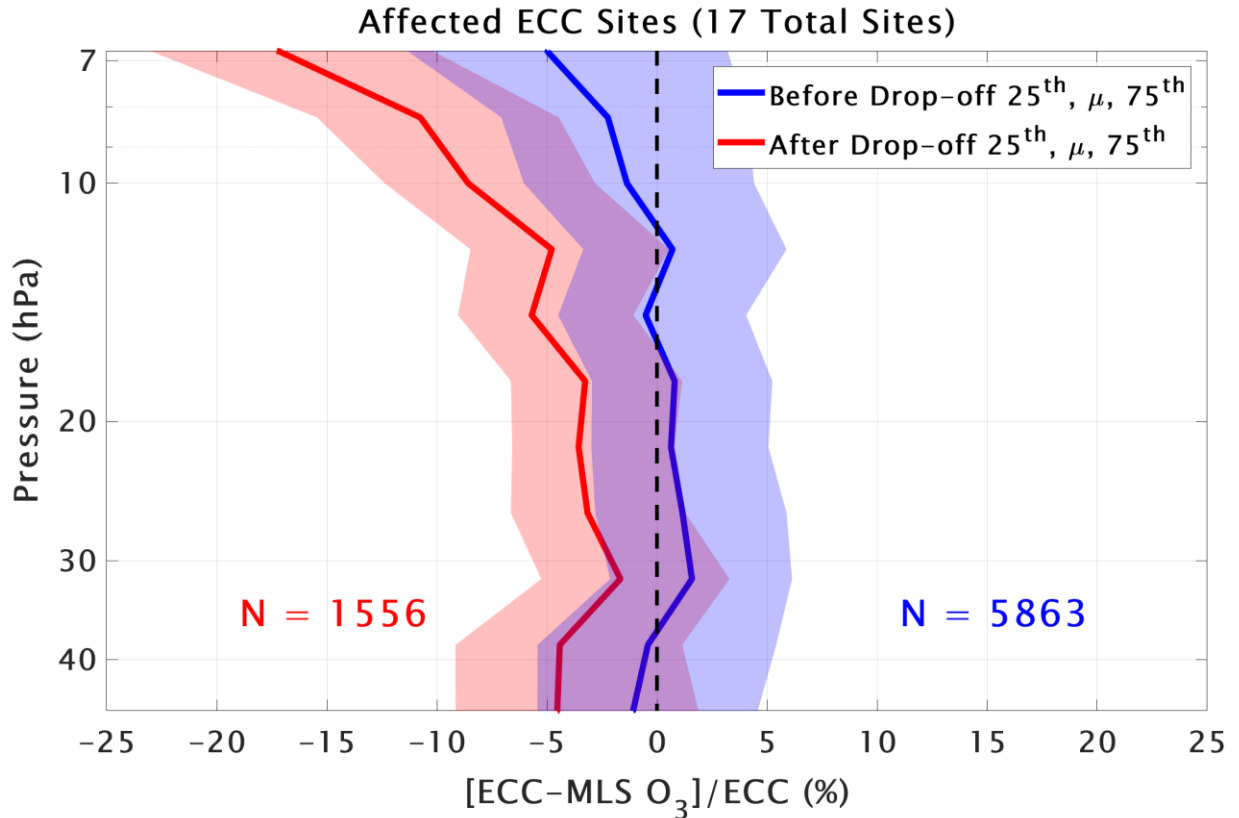
Site	ECC	N	Lat (°)	Lon (°)	KI SST	OMI 25th (%)	OMI μ (%)	OMI 75th (%)	Drop-Off	TCO Drop (%)	Ground TCO
Alert	Type1	645	82.49	-62.34	1.0%, Full	-0.6	1.0	3.1	02/2016	-3.6	Brewer
Eureka	Type1	922	79.98	-85.94	1.0%, Full	-0.4	1.9	4.5	01/2016	-2.4	Brewer
Resolute	Type1	540	74.7	-94.96	1.0%, Full	-4.8	-2.2	0.6	03/2015	-4.4	Brewer
Churchill	Type1	417	58.74	-94.07	1.0%, Full	-1.1	0.7	3.3	06/2016	-7.5	Brewer
Edmonton	Type1	674	53.54	-114.1	1.0%, Full	-2.9	-0.4	2.9	08/2016	-3.3	Brewer
Goose Bay	Type1	663	53.31	-60.36	1.0%, Full	-1.9	0.7	3.4	N/A	N/A	Brewer
De Bilt	Type2	736	52.1	5.18	1.0%, Full	-0.6	1.3	2.9	N/A	N/A	Brewer
Uccle	Type1	2140	50.8	4.35	0.5%, Half	-1.5	0.0	2.0	N/A	N/A	Brewer
Kelowna	Type1	664	49.93	-119.4	1.0%, Full	1.4	3.4	5.9	03/2015	-4.4	N/A
Payerne	Type1	2191	46.49	6.57	0.5%, Half	-2.5	-0.7	0.9	N/A	N/A	N/A
Yarmouth	Type1	616	43.87	-66.11	1.0%, Full	-0.2	2.4	5.3	04/2016	-8.2	N/A
Sapporo	Type1	373	43.06	141.33	0.5%, Half	1.0	2.7	4.4	N/A	N/A	Dobson
Trinidad Head	Type1	772	40.8	-124.16	1.0%, 1/10	-2.1	-0.2	1.6	N/A	N/A	N/A
Madrid	Type2	680	40.47	-3.58	1.0%, Full	-2.1	-0.3	1.6	N/A	N/A	Brewer
Boulder	Type1	816	40	-105.25	1.0%, 1/10	-2.1	-0.3	2.0	N/A	N/A	Dobson
Wallops Island	Type2	773	37.93	-75.48	1.0%, Full	-2.5	-0.3	1.8	N/A	N/A	Dobson
Tateno	Type1	430	36.06	140.13	0.5%, Half	0.8	2.6	4.3	N/A	N/A	Dobson, Brewer
Huntsville	Type1	759	34.72	-86.64	1.0%, 1/10	-1.6	0.0	1.9	N/A	N/A	N/A
Naha	Type1	403	26.21	127.69	0.5%, Half	0.2	1.7	3.5	N/A	N/A	Dobson
Hong Kong	Type2	690	22.31	114.17	1.0%, Full	-7.0	-4.6	-2.1	N/A	N/A	N/A
Hanoi	Type1	264	21.01	105.8	0.5%, Half	-4.1	-1.8	0.5	11/2014	-2.6	N/A
Hilo	Type1	711	19.43	-155.04	1.0%, 1/10	-3.7	-1.9	0.2	08/2014	-3	Dobson, Brewer
Costa Rica	Type1	605	9.94	-84.04	1.0%, 1/10	-3.1	-0.8	1.9	01/2016	-5.5	N/A
Paramaribo	Type2	517	5.8	-55.21	1.0%, Full	-5.0	-2.5	-0.1	N/A	N/A	Brewer
Kuala Lumpur	Type1	264	2.73	101.27	0.5%, Half	-7.3	-4.5	-1.3	N/A	N/A	N/A
San Cristobal	Type1	168	-0.92	-89.62	1.0%, 1/10	-4.9	-0.8	2.4	08/2013	-5.2	N/A
Nairobi	Type1	596	-1.27	36.8	0.5%, Half	-3.7	-2.1	-0.4	06/2015	-2.2	N/A
Natal	Type2	400	-5.42	-35.38	1.0%, Full	-3.6	-1.5	1.0	09/2013	-2.7	Dobson
Watukosek	Type1	115	-7.5	112.6	2.0%, None	-3.4	-1.9	0.4	N/A	N/A	N/A
Ascension	Type1	394	-7.58	-14.24	0.5%, Half	-6.0	-2.8	0.4	03/2016	-3.3	N/A
Samoa	Type1	474	-14.23	-170.56	1.0%, 1/10	-3.0	-1.2	0.9	01/2017	-3.1	Dobson
Fiji	Type1	200	-18.13	178.4	1.0%, 1/10	-3.1	-0.5	2.2	12/2015	-4	N/A
Réunion	Type1	449	-21.06	55.48	0.5%, Half	-2.0	0.3	2.4	N/A	N/A	SAOZ
Irene	Type2	212	-25.9	28.22	1.0%, Full	-1.3	1.3	4.3	N/A	N/A	Dobson
Broadmeadows	Type2	667	-37.69	144.95	1.0%, Full	-0.9	0.6	2.7	N/A	N/A	Dobson
Lauder	Type1	705	-45	169.68	0.5%, Half	-3.3	-1.3	0.8	09/2016	-2.2	Dobson
Macquarie	Type2	675	-54.5	158.95	1.0%, Full	-4.6	-2.4	0.1	N/A	N/A	Dobson



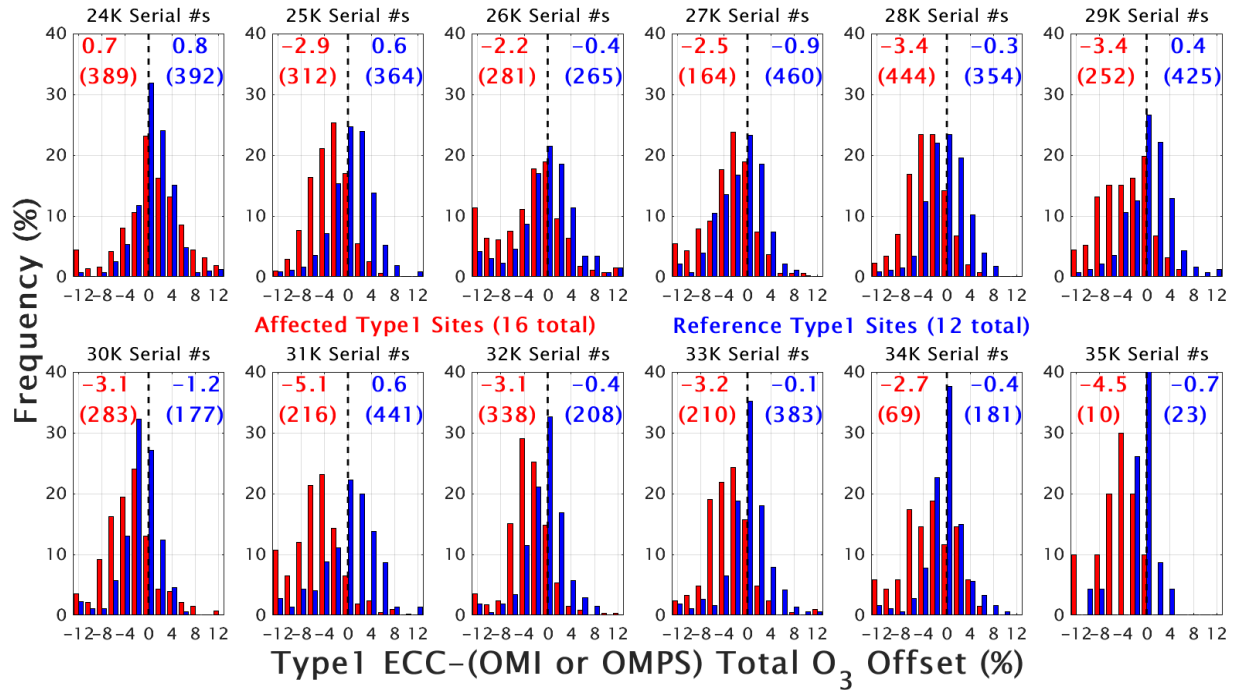
436
 437 Figure 1. Time series of comparisons at Kelowna (A; data end in June 2017), Nairobi (B), and
 438 Lauder (C) between ECC ozonesondes and Aura MLS stratospheric O₃ profiles (top panels), and
 439 OMI (blue dots) and OMPS (red dots) TCO (bottom panels). Red or blue colors on the top panels
 440 indicate where the ECC O₃ is greater or less than MLS. Horizontal dashed lines indicate the 0 %
 441 line for TCO comparisons. Vertical dashed lines indicate the beginning of the low bias at each
 442 site (see Table 1 for dates), marked by a sudden drop in O₃ relative to satellite measurements.
 443



444
 445 Figure 2. Map of all 37 ECC ozonesonde sites considered in this study. The blue dots indicate
 446 sites that show no detectable TCO drop-off relative to OMI TCO. We call these sites “reference”
 447 sites. The orange, red, and purple dots indicate sites that exhibit drops of 2-4 %, 4-6 %, and over
 448 6 % relative to OMI TCO. The method for computing the values shown on this figure and in
 449 Table 1 are explained in Section 2.3.
 450



451
 452 Figure 3. A composite of comparisons between ECC ozonesonde and Aura MLS stratospheric O₃
 453 profiles from before the drop-off at each site (blue; dates of drop-off are in Table 1), and during
 454 the period after the drop-off (red). The shading indicates the 25th to 75th percentile, with mean
 455 values shown by the solid lines. ECC sonde sample numbers are shown for each period in the
 456 lower portion of the figure.
 457



458

459

460

461

462

463

464

465

466

467

468

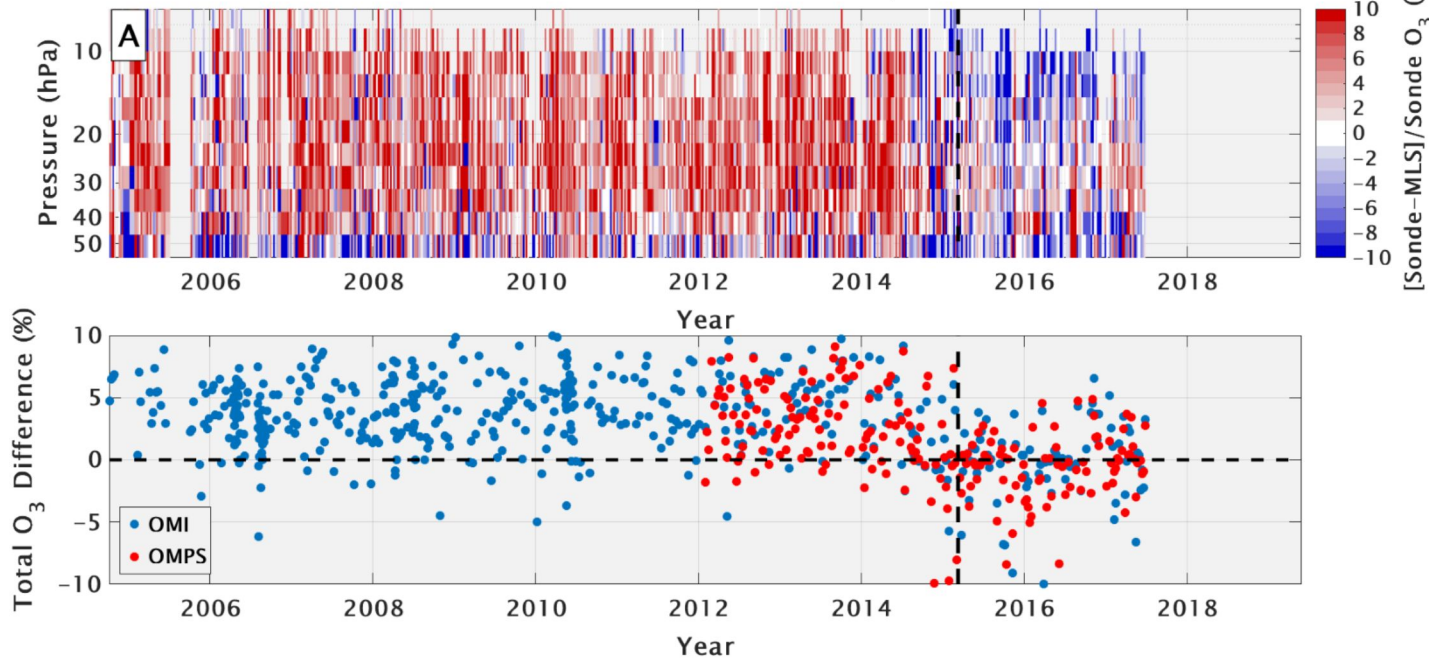
469

470

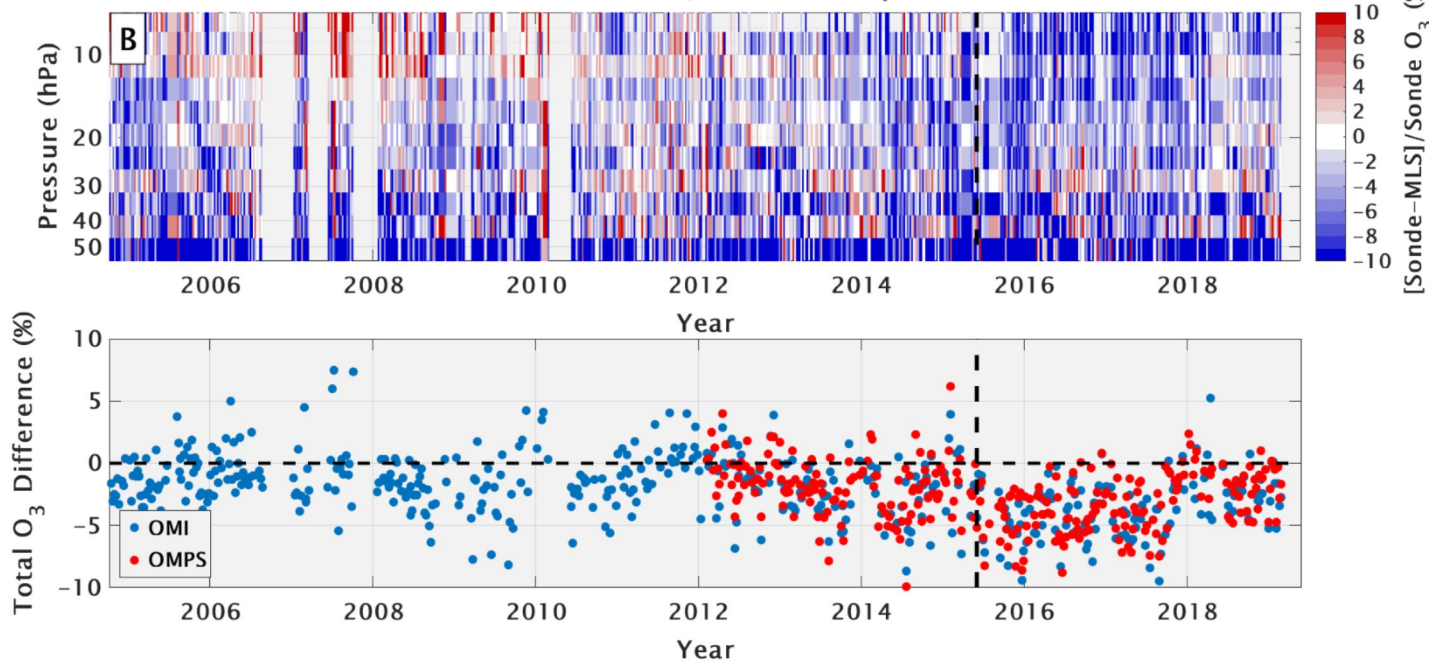
Figure 4. Histograms of Type1 ECC ozonesonde comparisons with OMI and OMPS TCO in percent difference (ECC-satellite/ECC). Comparisons are separated into every 1000 serial numbers from 24000 to 35000, and by sites affected (red) and reference (blue) by the ozonesonde drop-off. Data are binned every 2 % from -12 to 12 %. The median percent difference for each set is listed at top of the panels, with the total number of comparisons with OMI and OMPS in parentheses. For example, Type1 31000s serial numbers at affected sites have a median bias of -5.1 % compared to OMI and OMPS, with 216 total ECC/satellite comparisons (sondes are double-counted for comparison to both OMI and OMPS overpasses). Reference site Type1 31000s serial numbers have a median bias of +0.6 %, with 441 total ECC/satellite comparisons.

Figure1.

Kelowna Ozonesonde, Satellite Comparisons



Nairobi Ozonesonde, Satellite Comparisons



Lauder Ozonesonde, Satellite Comparisons

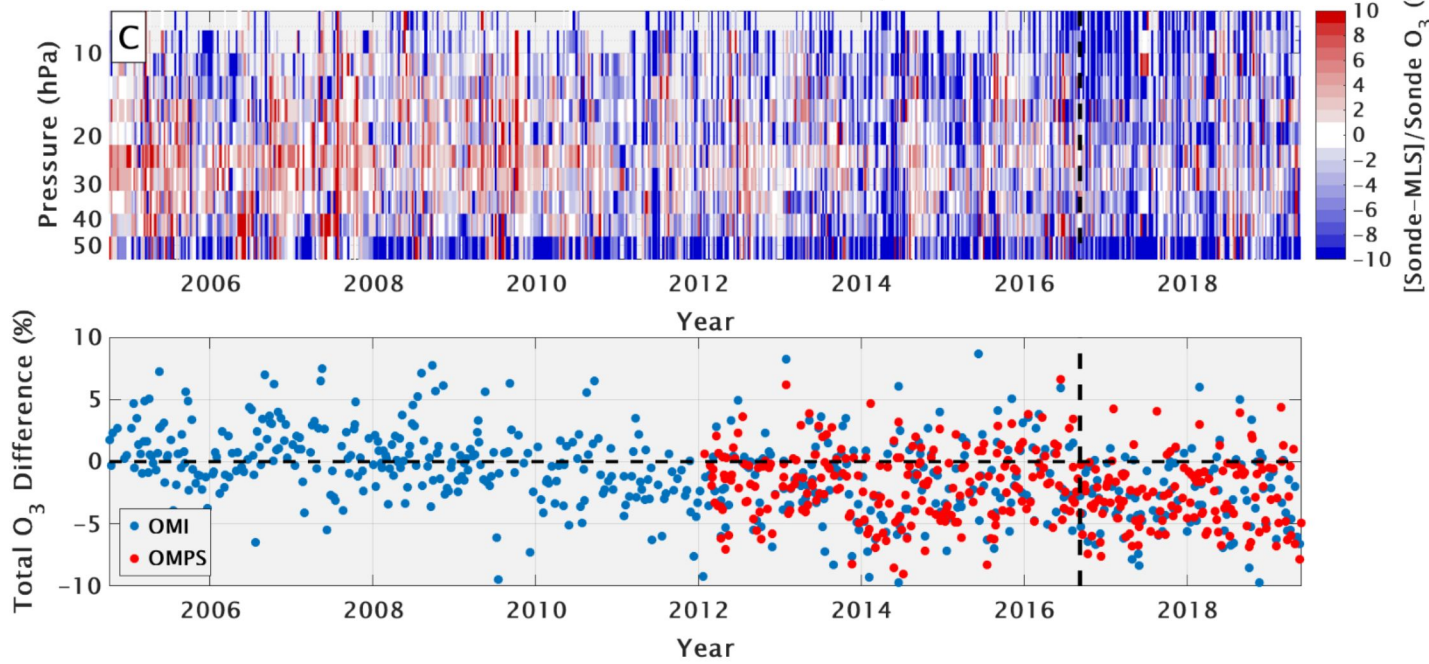


Figure2.

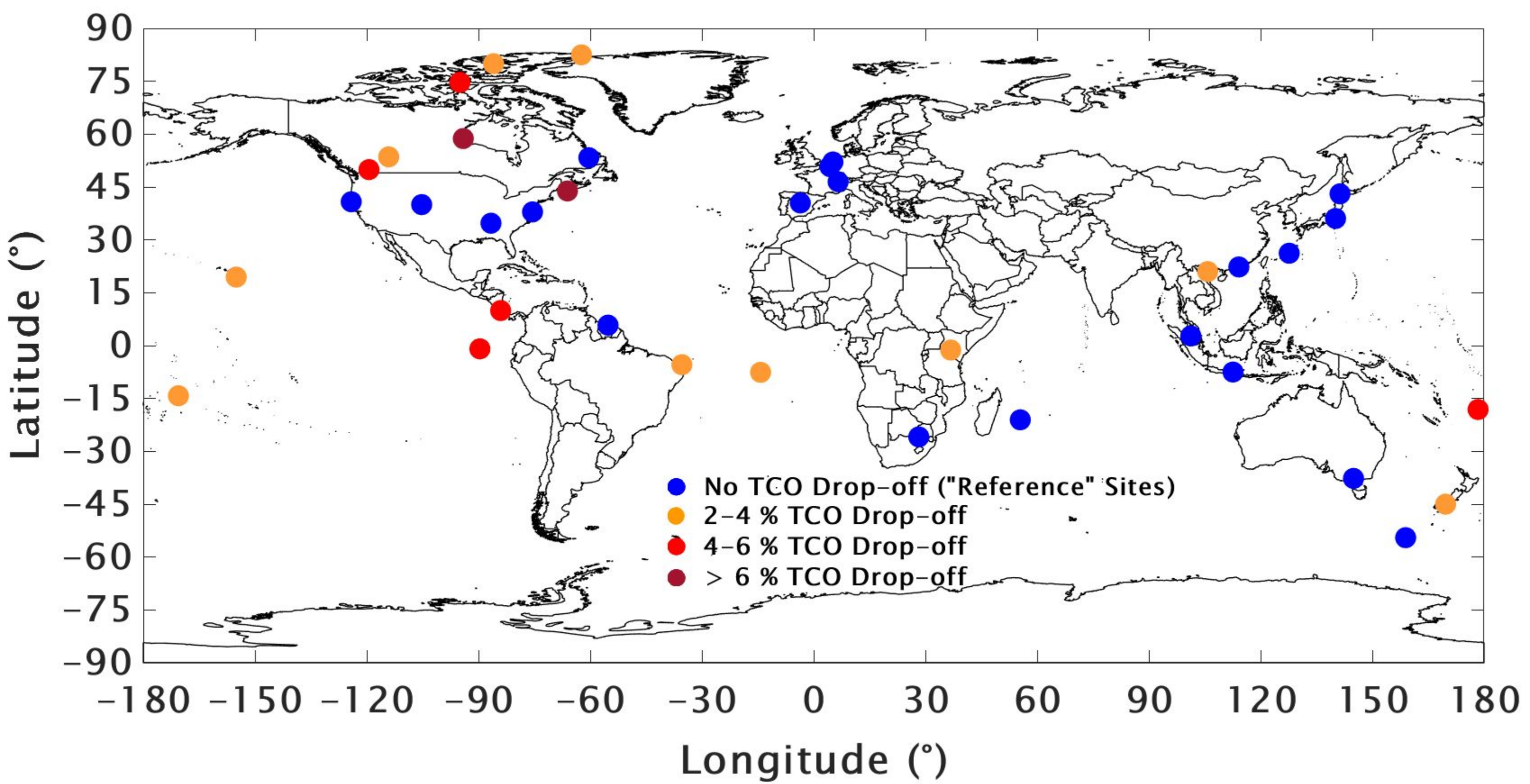


Figure3.

Affected ECC Sites (17 Total Sites)

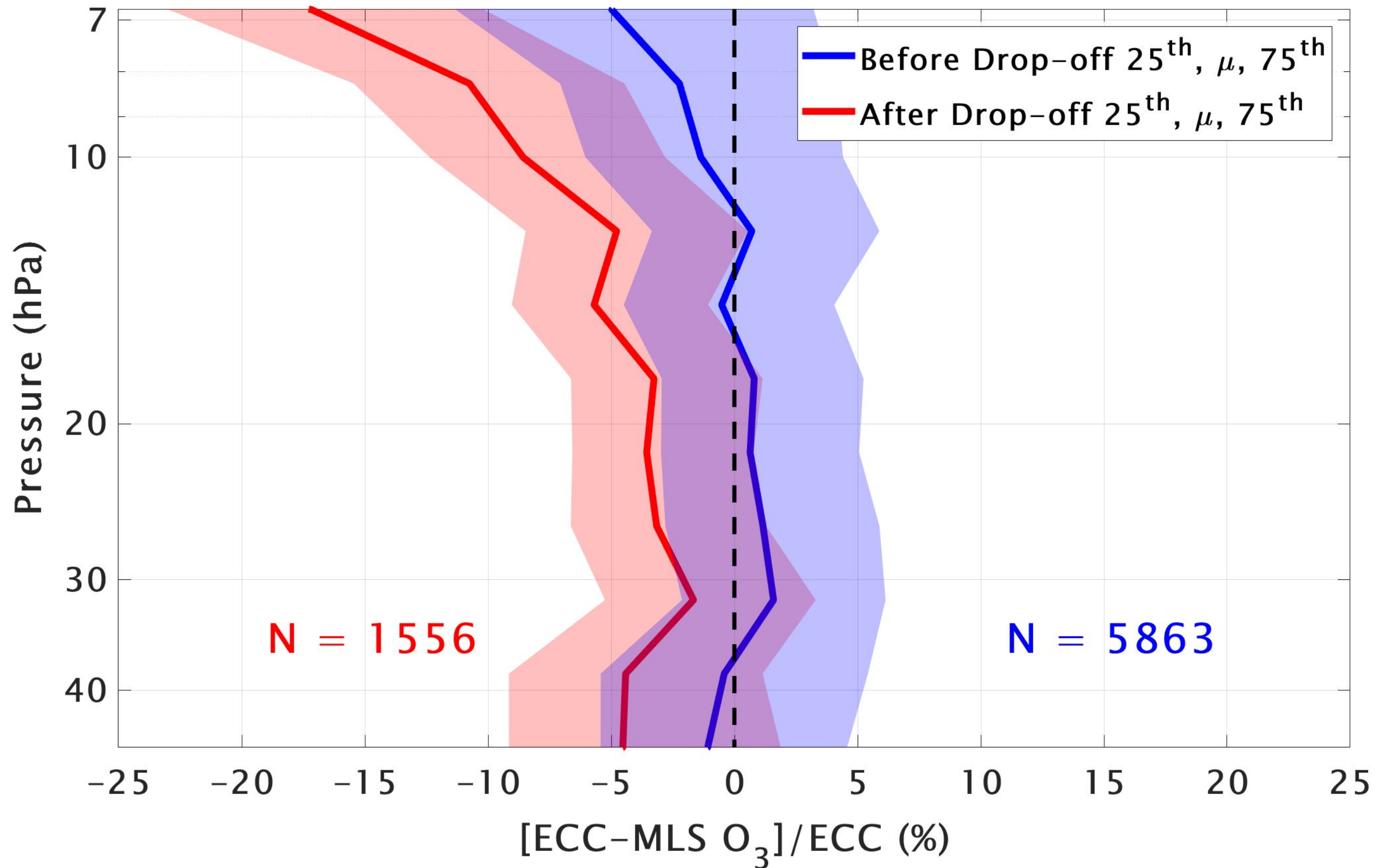


Figure4.

